UC Irvine
UC Irvine Previously Published Works

Title

CD133 Expression Correlates with Membrane Beta-Catenin and E-Cadherin Loss from Human Hair Follicle Placodes during Morphogenesis

Permalink

https://escholarship.org/uc/item/0k65d026

Journal

Journal of Investigative Dermatology, 135(1)

ISSN

0022-202X

Authors

Gay, Denise L
Yang, Chao-Chun
Plikus, Maksim V
et al.

Publication Date

2015

DOI

10.1038/jid.2014.292

Peer reviewed

CD133 expression correlates with membrane beta-catenin and e-cadherin loss from human hair follicle placodes during morphogenesis

Denise Gay[1,2], **Chao-Chun Yang**[1,3], **Maksim Plikus**[4], **Mayumi Ito**[5], **Charlotte Rivera**[1], **Elsa Treffeisen**[1], **Laura Doherty**[1], **Michelle Spata**[1], **Sarah E. Millar**[1,6], and **George Cotsarelis**[1]

[1]Department of Dermatology, University of Pennsylvania, Philadelphia, PA, USA

[3]Department of Dermatology, National Cheng Kung University Hospital, College of Medicine, National Cheng Kung University, Tainan, Taiwan

[4]Department of Developmental and Cell Biology, Sue and Bill Gross Stem Cell Research Center, University of California, Irvine, CA, USA

[5]Department of Dermatology, New York University Langone Medical Center, New York, NY, USA

[6]Department of Cell and Developmental Biology, University of Pennsylvania, Philadelphia, PA, USA

Abstract

Genetic studies suggest that the major events of human hair follicle development are similar to those in mice, but detailed analyses of this process are lacking. In mice, hair follicle placode 'budding' is initiated by invagination of Wnt-induced epithelium into the underlying mesenchyme. Modification of adherens junctions is clearly required for budding. Snail-mediated downregulation of adherens junction component E-cadherin is important for placode budding in mice. Beta-catenin, another adherens junction component, has been more difficult to study due to its essential functions in Wnt signaling, a prerequisite for hair follicle placode induction. Here, we show that a subset of human invaginating hair placode cells expresses the stem cell marker CD133 during early morphogenesis. CD133 associates with membrane beta-catenin in early placodes and its continued expression correlates with loss of beta-catenin and E-cadherin from the cell membrane at a time when E-cadherin transcriptional repressors Snail and Slug are not implicated. Stabilization of CD133 via anti-CD133 antibody treatment of human fetal scalp explants depresses beta-catenin and E-cadherin membrane localization. We discuss this unique correlation and suggest a hypothetical model whereby CD133 promotes morphogenesis in early hair follicle placodes through the localized removal of membrane beta-catenin proteins and subsequent adherens junction dissolution.

Corresponding author: George Cotsarelis, M.D., Department of Dermatology, Perelman School of Medicine, University of Pennsylvania, Philadelphia, PA, USA 19104, cotsarel@mail.med.upenn.edu.
[2]Current address UMR 967 CEA-INSERM, Fontenay-aux-Roses, France

Conflict of interest
None.

Introduction

In mice, hair follicle placode induction and early morphogenesis require spacial and temporal activation cues, of which Wnt activation is the earliest known signal. This is followed by activation of Eda:Edar, TGF-beta, Sonic Hedgehog and other signaling pathways to prompt organ downgrowth and differentiation (Chiang et al, 1999; Millar, 2003; Mikkola, 2007). The first shape modifications defining the new placode from adjacent interfollicular epidermis include elongation and cell membrane apical curvature promoting invagination of Wnt-activated cells.

Adherens junctions (AJs), required for tight cell:cell contacts, undergo considerable remodeling during skin and hair morphogenesis and their proteins, in particular E-cadherin and beta-catenin, have been well studied in this regard (Stepniak et al, 2009; Heuberger and Birchmeier, 2010).

E-cadherin downmodulation appears to be a critical event in early 'budding' morphogenesis, and its downregulation is a well-known early step in hair placode morphogenesis (Müller-Röver et al, 1999; Jamora et al, 2003; Tinkle et al, 2003; Tinkle et al, 2008). It has been shown that E-cadherin may be downregulated via one of several mechanisms. First, its' transcription can be negatively regulated by Twist and Snail/Slug transcriptional modifiers (reviewed by Peinado et al, 2007), which are in turn targets of Wnt and/or TGF-beta activation (Jamora et al, 2005; ten Berge et al, 2008). Hair follicle budding morphogenesis has been shown to depend upon this pathway in mice albeit later then the earliest stages of cell curvature and invagination (Jamora et al, 2005, Devenport and Fuchs, 2008). Alternatively, E-cadherin protein can be down-modulated at the cell membrane and several adhesion proteins and planar polarity proteins, including EpCAM, have been implicated in this process, although none has been shown to have a role in hair follicle budding morphogenesis (Shtutman et al, 2006; Litvinov et al, 1997; Warrington et al, 2013).

Beta-catenin is a component of AJs, linking E-cadherin to the underlying cytoskeleton. Although the relative importance of beta-catenin to AJs during skin development has been directly addressed in conditional beta-catenin knockouts, its role has been difficult to establish because related family member plakoglobin can partially compensate for its loss (Huelsken et al, 2001). Examining a role for beta-catenin in hair follicle development has been further impeded because placode induction requires Wnt activation, of which beta-catenin is an essential component. Thus knockouts lack even the earliest formation of placodes (Huelsken et al, 2001; Andl et al, 2002; Zhang et al, 2008).

CD133, a pentaspan membrane glycoprotein, is a well known stem cell marker in hematopoietic and neural tissues, and is also expressed on progenitor cells and simple luminal epithelia in a number of tissues (Florek et al, 2005; Karbanova et al, 2008). Although widely studied, its function remains unclear (Corbeil, 2013; Grosse-Gehling et al, 2013). Recently, CD133-knockout mice were shown to exhibit reduced mammary gland ductal branching, suggesting a possible role in tube morphogenesis (Anderson et al, 2012). In an unrelated study, it was shown that CD133 can interact with the histone deacetylase

HDAC6 at the cell membrane to reduce membrane beta-catenin and stabilize it via deacetylation for increased Wnt activation in human cells (Mak et al, 2012).

We have found that CD133 is expressed in early human hair follicle placodes and that its expression correlates with membrane beta-catenin and E-cadherin down modulation. Based upon these and related studies, we propose a potential model for AJ disassembly during early human placode morphogenesis through the down modulation of membrane beta-catenin by CD133.

Results

CD133 expression defines a subpopulation of cells in the developing human hair follicle placode

In analyzing expression of various markers in human epidermis during fetal development, (embryonic week 12–14), we found that CD133 (prominin 1) localized to a subpopulation (2%) of alpha6-integrin[+]EpCAM-high basal cells (Fig. 1a). In agreement with Ito et al (2007), we found no CD133 expression in embryonic mouse follicular or interfollicular epidermal cells, indicating this expression pattern is unique to humans (Fig. S1).

Confocal analyses of 12 week fetal epidermis whole mounts showed that EpCAM and CD133 colocalized on early hair follicle placodes (Fig. 1b) (Anti-CD133 antibodies AC133 and 293C3 showed identical staining patterns in human fetal scalp (see Fig. S2)). EpCAM expression appeared to precede that of CD133 because EpCAM-only placodes could be observed at this early time point (Fig. 1b left panel) whereas placodes at later times always expressed both markers. Immunofluorescence (IF) analyses of fetal skin cross-sections and confocal image stacks of entire placodes showed that CD133 co-localized with EpCAM along apical and lateral cell:cell boundaries (Fig. 1c, d). During hair follicle development, CD133 expression appeared to shift from early basal localization to redistribution along apical and lateral junctions with some retention of the protein at basal junctions in hair germs (Fig. 1e). CD133 expression decreased dramatically at later times suggesting that its functions are limited to early placode development.

CD133 expression correlates with Wnt activation and morphogenesis but not proliferation

To precisely delineate the stages of hair follicle development associated with CD133 expression, we compared its localization with a panel of proteins known to be important for mouse placode induction and subsequent morphogenesis (Fig. 2a, b, c). Canonical Wnt activation is an important induction event in mouse hair follicle development (Andl et al, 2002; Zhang et al, 2008). CD133 expression correlated with Wnt activation as determined by translocation of beta-catenin to nuclei and expression of Wnt target LEF1 in early human hair follicle placodes (Fig. 2a, top panels). Key morphogenetic regulators, TGF-beta and Wif1, were also observed in CD133^{+} cells (Fig. 2a) (Jamora et al, 2005; Surmann-Schmitt, 2009).

Surprisingly, Ki-67, a nuclear marker for proliferating cells, only infrequently co-localized with CD133-expressing cells in early placodes (Fig. 2a). Triple staining for Ki-67, CD133

and Lef1 confirmed that early placodes had undergone Wnt activation but remained relatively quiescent (Fig. 2c and Fig. 2d for quantitation).

Early budding morphogenesis is characterized by AJ remodeling and E-cadherin down-modulation, allowing for cell movement and shape changes concurrent with invagination. In agreement with studies on murine hair follicle morphogenesis (Muller-Rover et al, 1999), E-cadherin was downregulated and a related cadherin, p-Cadherin, upregulated at this timepoint (Fig. 2a).

Snail, an important down regulator of E-cadherin transcription, was not found in early placodes (Fig. 2a,b and Fig. S3), although in agreement with previous reports (Jamora et al, 2005; Devenport and Fuchs, 2008), hair germs expressed activated nuclear Snail (Fig. 2b). Slug, a close relative of Snail also implicated in E-cadherin transcriptional regulation (Bolos et al, 2002), was present in the cytoplasm of many basal cells including early placodes however nuclear localization of activated Slug was rare (Fig. 2a,b and Fig. S3). Thus, down-modulation of membrane E-cadherin did not appear to result from transcriptional repression by Snail/Slug family members.

TEM analyses confirmed the existence of many gaps at apical and lateral cell-cell junctions along invaginating basal cells within placodes, supporting the concept that these cells are actively engaged in junctional remodeling (Fig. 2e). Other reports, examining desmosomal systems in early mouse placodes, also showed a paucity of placode but not interfollicular desmosomes, further supporting this concept (Nanba et al, 2000).

CD133+ cells express genes implicated in early hair follicle placode morphogenesis and related EMT

To better define the role of CD133+ cells in placode development, 13 week fetal scalp epidermal cells were sorted for expression of CD133 and alpha6-integrin (Fig. 3a) and RNA subjected to microarray analyses. As expected, alpha6-integrin+CD133− (ITGA6+) and α6-integrin+CD133+ double positive (CD133+) populations, both of epidermal basal origin, shared expression of many genes (Fig. 3b Venn diagram). Fig. 3c shows a heatmap comparing differences in gene expression by ITGA6+ and CD133+ populations.

As anticipated, multiple activation pathways were upregulated in the CD133+ population, in agreement with those previously defined as important for murine hair follicle development (Table 1, Millar, 2003; Lee and Tumbar, 2012). Independent bioinformatics analyses also revealed upregulation of overlapping gene sets in the CD133+ population associated with morphogenesis and related EMT functions, in particular those associated with signaling and cell motility. And genes associated with cell:cell adhesion were downregulated. Interestingly, no known EMT transcriptional modifier of e-cadherin was upregulated and targets of these modifiers were not downregulated, including CDH1, CDH2, vimentin and fibronectin, in the CD133+ population (Table 1).

Array analyses and QPCR of ITGA6+ and CD133+ populations (Table I and Fig. 3d) confirmed IF data (Fig 2a) that CD133+ cells had undergone Wnt activation and served as a primary source of TGF-beta2, Wif1 and Slug (SNAI2) transcription. As mentioned above,

CDH1 (e-cadherin) gene expression was not downregulated (Table 1) although protein expression was clearly downregulated in CD133^{+} cells (Fig. 2a). QPCR confirmed that Snail (SNAI1) transcription was essentially absent from CD133^{+} cells whereas Slug (SNAI2) was expressed by both ITGA6^{+} and CD133^{+} populations (Fig 3d). Observations that inactive Slug localized to cytoplasm rather than the nucleus in IF analyses (Fig. 2a,b and Fig S3) were supported by the fact that Slug downregulated gene targets like CLDN1 were upregulated in CD133^{+} cells (Table 1, Martínez-Estrada et al, 2006).

These combined results suggest that although CD133^{+} cells engage in budding morphogenesis and express downstream genes associated with this (and shared with EMT-mediated morphogenesis), EMT regulators do not initiate this event.

CD133 colocalizes with AJ proteins in early hair placodes and localizes to regions with decreased membrane beta-catenin and E-cadherin in more mature placodes

To investigate whether CD133 localized specifically to cell:cell junctions, fetal scalp epidermis was subjected to brief trypsinization and mechanical disruption to disengage placode and sub-placode clusters from surrounding interfollicular epidermis for more detailed viewing. CD133 colocalized with EpCAM along cell membranes and appeared to localize specifically to cell:cell junctions (Fig. 4a).

To determine which types of junctions CD133 might associate with, we undertook IF analyses. CD133 clearly localized to areas rich in E-cadherin during early placode curvature and, later, localized specifically to regions with downregulated E-cadherin expression (Fig. 4b). In contrast, CD133, as has been previously reported for EpCAM (Lei et al, 2012; Wu et al, 2013), did not localize to TJs as determined by ZO1 co-staining (Fig. 4c).

CD133 has been reported to co-associate with HDAC6 and beta-catenin proteins at cell membranes (Mak et al, 2012). Because membrane beta-catenin is an essential constituent of AJs, we studied whether CD133 colocalized with beta-catenin on placode cell membranes. IF confirmed their colocalization during early placode morphogenesis (Fig. 4d). We also confirmed that HDAC6 is broadly expressed in the cytoplasm of epidermal cells and specifically colocalizes with CD133 along cell membranes (Fig. 4e).

To establish that CD133 associates with specific membrane proteins, and because co-IP analyses would be difficult given the low percentage of CD133^{+} cells in fetal epidermis, in situ proximity ligation (PLA) technology was employed. PLA analyses supported the idea that CD133 protein specifically bound EpCAM, beta-catenin and HDAC6 but not E-cadherin in placodes (Fig. 4f, red dots correspond to areas of specific protein:protein interaction. See Fig S4 for negative single antibody staining). Additional IF analyses to independently locate beta-catenin or HDAC6 and CD133 further confirmed these observations (Fig. 4f), however the low incidence of CD133:HDAC6 interaction suggested that it may be transient.

CD133 has been implicated in loss of beta-catenin from cell membranes (Mak et al, 2012). Because beta-catenin is highly abundant in epidermis, potential changes in its membrane expression might not be detected by conventional IF microscopy. To analyze this, confocal

microscopy of whole placodes co-stained for CD133, E-cadherin and beta-catenin was undertaken. Fig 4g shows a typical early placode, with some CD133:beta-catenin colocalization (pink arrowhead). However, overall, CD133-rich membranes exhibited decreased beta-catenin localization (Fig 4g, white arrowheads). Quantitation of levels of beta-catenin along CD133-positive and -negative membranes confirmed this observation (Fig 4h). Tight localization of E-cadherin to cell junctions, which could be easily observed in CD133-negative regions, was also lost (Fig 4g, right panels, white arrowheads).

To analyze CD133 protein localization in detail, silver enhanced gold-particle IFTEM analyses were undertaken. Initial IF analyses showed good labeling of anti-CD133 treated placodes and thus good penetration into tissue (Fig. S5). IFTEM analyses showed specific localization of gold particles to regions typically rich in AJs, near or in gaps along lateral and apical cell:cell junctions (Fig. 4i). Immunogold also localized infrequently to intracellular vesicles suggesting that CD133 expression is regulated via endosomal trafficking (Fig. 4i).

Anti-CD133 antibody increases down-modulation of cell membrane beta-catenin and E-cadherin in human fetal scalp explants

To directly address a function for CD133, we studied fetal scalp explants (Fig. 5a for schematic and Materials and Methods for culture details and potential caveats). Explants cultured for 16–20 hours retained good morphology and development, as evidenced by continued follicle growth (Fig. 5b), however at later times, epidermal structure became disorganized.

The unavoidable short culture duration prevented us from undertaking knockdown experiments with siRNAs or viruses to address long-term effects such as morphologic or transcriptional alterations. Therefore, explants were cultured short-term with anti-CD133 antibodies to address potential changes in membrane E-cadherin and beta-catenin expression. Anti-CD133 antibody or an isotype control antibody was applied to explants at Day 0 and explants analyzed at 20 hours. Comparison of anti-CD133-treated and control explants showed that anti-CD133 antibody permeated well into placodes during the culture period (Fig. 5c). Also, comparisons of Day 0 placodes and anti-CD133 explant placodes showed that antibody treatment over time resulted in increased CD133 surface expression, suggesting that antibody binding prevented CD133 protein internalization (Fig. 5c,d).

Explants were analyzed for expression of membrane E-cadherin protein. Surprisingly, anti-CD133 explant placodes showed markedly reduced E-cadherin expression throughout the entire placode compared with controls (Fig. 5e and Fig. 5f for quantitation).

Infrequently, placodes that had received less CD133 antibody during culture were observed. These placodes resembled those treated with control antibody, whereas placodes with increased CD133 antibody binding showed dysregulated EpCAM localization as well as reduced membrane E-cadherin expression (Fig. 5g).

Stacked confocal images further demonstrated differences between anti-CD133-treated and control explants in both EpCAM and E-cadherin localization (Fig. 5h, lower left panel was

enhanced to show membrane localization of E-cadherin. Insets show unenhanced views). As anticipated, examination of beta-catenin in anti-CD133 explants showed extensive loss of beta-catenin from membranes specifically in regions of CD133 localization (Fig. 5i).

Discussion

Here, we have observed a striking correlation between localized CD133 expression and downmodulation of AJ proteins during human hair follicle placode morphogenesis. CD133 is expressed on the apical and lateral cell membranes of a subpopulation of invaginating basal cells during early placode morphogenesis. CD133 physically associates with membrane beta-catenin and its localization correlates specifically with loss of membrane beta-catenin and E-cadherin in later placodes. Anti-CD133 antibody treatment augments this loss presumably through stabilization of CD133 protein. Given its temporal and regional localization in early placodes and its enhanced function in anti-CD133 explants, we have proposed a hypothetical model suggesting that CD133 may be involved in down modulatation of membrane beta-catenin for the destabilization of AJs during early human hair follicle morphogenesis (see model, Fig. 6).

Our model supports the concept that CD133 functions primarily during stage I placode formation, ie after Wnt and Eda/Edar signaling but before induction of e-cadherin transcriptional regulators (Millar, 2003; Schneider et al, 2009). We found no role for Snail or Slug during the earliest steps in human placode morphogenesis. However, activated nuclear Snail and Slug were observed in more differentiated hair germs, as previously reported in mice (Jamora et al, 2005; Devenport and Fuchs, 2008). Therefore, we suggest that the first step in AJ disruption in human placodes at least, may be at the level of membrane E-cadherin protein down-modulation, followed by Snail/Slug-mediated E-cadherin transcriptional down-regulation. Snail/Slug family members are target genes of Wnt and TGF-beta pathways (Jamora et al, 2005; ten Burge et al, 2008) and indeed Slug expression was evident in early human placodes. However, nuclear localization, indicating activation, was rare. We suggest that requisite cues for snail/slug activation may be limiting during this early period.

Whether CD133 participates with HDAC6 in the deacetylation of beta-catenin remains unknown but CD133 and HDAC6 do co-associate in early placodes suggesting this as a possibility. Mak et al (2012) showed that HDAC6-mediated beta-catenin deacetylation can upregulate Wnt activity and subsequent proliferation in cell lines. We have not observed proliferation of CD133^{+} cells in early human placodes, however, CD133^{+} cells have undergone at least some Wnt activation as evidenced by nuclear localization of beta-catenin and gene expression of Wnt targets. This suggests that either a threshold of activity has not been met for proliferation or that Wnt activity may not lead to proliferation of these cells. Recent work by Hirata et al (2013) has demonstrated that high levels of Wnt activation can result in the maintenance rather than the proliferation of colonic epithelial stem cells.

PLA analyses showed that CD133 and EpCAM proteins directly associate and may have linked functions. This is not surprising given that they are found on many of the same cells including luminal epithelial precursors and stem cells (Karbanova et al, 2008; Trzpis et al,

2008). In early reports, EpCAM was postulated to directly influence E-cadherin expression and AJ stability in transfected cell lines (Litvinov et al, 1997). In agreement with recent reports, we do not find a direct role for EpCAM in E-cadherin regulation in human hair follicle placodes (Lei et al, 2012; Wu et al, 2013). EpCAM is broadly expressed throughout the placode rather than specifically in regions of E-cadherin down-regulation and its aggregation in anti-CD133 explants does not correlate with E-cadherin and beta-catenin loss.

In these studies, we have shown that humans and mice exhibit many similarities and some differences in hair follicle placode morphogenesis. Wnt activation and later signaling pathways appear to be common to both. However, CD133 is expressed only in human hair follicle placodes indicating that its function is unique to human hair development. Thus, our results underscore the significant differences that can exist between humans and other mammals and stress the importance of human models.

Materials & Methods

Human Tissue procurement

Human fetal scalp was procured from Advanced Bioscience Resources, Inc. (ABR, Alameda, CA) in conformity with federal and state laws and following National Institute of Health Human Fetal Tissue Research Review Panel of 1988 guidelines. The gestation period was estimated by ABR based on testimonials and patient examination. We further distinguished age based on placode coverage (no placodes denoted tissue less then 11 weeks, partial placode coverage 11–12 weeks and complete coverage, 13 weeks and older). Any observance of external hair shafts defined the tissue as at least 14 weeks.

Prom1 Mice

Engineered mice containing a knockin of the creERT2-IRES-nlacZ cassette into the *Prominin 1* locus were kindly provided by Liqin Zhu and Richard Gilbertson (Zhu et al, 2009). Staining of mouse skin for beta galactosidase expression is as described by Gay et al (2013).

Antibodies

See Supplementary Table 1.

Epidermal cell isolation, flow cytometry and cell sorting

Epidermal cells were isolated using dispase II (Roche) at 4°C for 12 hours, followed by treatment with 0.25% trypsin/EDTA for 5 minutes. 4′,6-diamidino-2-phenylindole (DAPI) was used to exclude dead cells from analyses and sorting. We undertook FACS analyses using a FACSCanto A and cell sorting using a FACSVantage SE and FACSDiVa software and analyzed data with FlowJo software. Populations were sorted directly into Trizol LS (Life Technologies) for RNA isolation.

Immunohistochemistry

Briefly, frozen tissue sections were processed as described in Gay et al, 2013. Images were obtained using a Zeiss LSM 710 Confocal or Leica deconvoluting microscope and analyzed using ImageJ software (Abramoff, et al, 2004). Fluorescence intensities of individual cell membranes (Fig. 4h) were obtained by averaging plot profile lists using Fiji software (see Fig S6 for a representative analysis). Relative intensities were generated by setting the highest beta-catenin intensity for each placode to 1 and comparing data within and between placodes. In Fig. 5d and f, fluorescence intensities of entire placodes were compared.

Detailed immunohistochemistry procedures can be found in Supplementary Methods.

In situ Proximity Ligation Assay (PLA)

Frozen tissue sections were treated as for immunohistochemistry (see Supplementary Methods) using the following antibody combinations: anti-CD133/2 (1:200) and anti-EpCAM (1:2500) or anti-E-cadherin (1:4000), anti-CD133 C-term (1:400) and beta-catenin (1:15,000) or HDAC6 (1:1000), and further processed as recommended by the manufacturer (Duolink In Situ-Fluorescence, Sigma-Aldrich).

Micoarray and QPCR analyses

RNA isolation and QPCR were undertaken as previously described (Gay et al, 2013). Microarray services were provided by the University of Pennsylvania Molecular Profiling Facility using the GeneChip® Human Gene 1.0 ST Array (Affymetrix Inc.) as described in the Ambion WT Expression Manual. A GeneChip 3000 7G scanner was used to collect fluorescence signals. The results in Table 1 reflect combined results from 2 independent sorts.

Partek Genomics Suite (Partek Inc.) and GENE-E data analyses software (http://www.broadinstitute.org/cancer/software/GENE-E/) were used to generate gene lists and heat maps. Lists were mined for functional and shared gene sets using DAVID (**D**atabase for **A**nnotation, **V**isualization and **I**ntegrated **D**iscovery, Huang et al, 2009a, Huang et al, 2009b) and GSEA (Gene Set Enrichment Analysis) (Subramanian et al, 2005, Mootha et al, 2003) respectively. Verification of EMT genes was from compilations of gene sets (Groger et al, 2012; Humtsoe et al, 2012; Byers et al, 2013). GEO accession number: GSE58393.

TEM and IFTEM analyses

Scalp tissue was fixed, and for ImmunoTEM, incubated overnight with anti-CD133-biotin (Miltenyl), followed by incubation with 1.4nm streptavidin Alexa Fluor 488-fluoronanogold particles (Nanoprobes). Tissue was refixed for electron microscopic examination, embedded in EMbed-812 (Electron Microscopy Sciences, Fort Washington, PA) and thin sections were silver enhanced with an R-Gent SE-EM kit (Electron Microscopy Sciences). Sections were examined with a JEOL 1010 electron microscope fitted with a Hamamatsu digital camera and AMT Advantage image capture software.

Explants

Whole fetal scalp tissue was placed on a porous screen and partially submerged in DMEM/1% FCS/PS/lGlu to provide an air interface (see Fig. 5A). For optimal penetration, 25ul anti-CD133/1 (Miltenyl) or IgG2b control antibody (diluted to 5 ug/ml in DMEM) was overlaid onto air-exposed epidermis and another 25–30 ul injected into dermis. Explants were cultured at 37°C, 5% CO_2 for 20 hours then prepared for immunohistochemistry. An air interface technique was used because full liquid submersion resulted in dissociation of overlying epidermis. The air interphase technique has been used successfully for other explants of tissue normally fully submerged in vivo (Wells et al, 2010; Bull et al, 2011). Others have shown that air interface can accelerate barrier development in rats (Komuves et al, 1999), however human tissue used in these studies is developmentally 8–12 weeks from this stage and it remains unknown whether air interface might have a similar effect on human scalp development.

Statistical analyses

All statistical analyses were performed by two–tailed Student's *t* test using Excel (Microsoft). $P < 0.05$ was considered significant. All data are expressed as means ± s.e.m.

Supplementary Material

Refer to Web version on PubMed Central for supplementary material.

Acknowledgments

Abbreviations

AJ	Adherens Junction
DAPI	4′,6-diamidino-2-phenylindole
EpCAM	Epithelial Cell Adhesion Molecule
FACs	Flow Cytometry
HDAC	Histone Deacetylase
IF	Immunofluorescence
IFTEM	Immunofluorescence Transmission Electron Microscopy
PLA	Proximity Ligation Assay
QPCR	Quantitative Real-time Polymerase Chain Reaction
TEM	Transmission Electron Microscopy

TJ	Tight Junction
TGF	Transforming Growth Factor

References

Abramoff MD, Magalhaes PJ, Ram SJ. Image Processing with ImageJ. Biophotonics International. 2004; 11:36–42.

Anderson LH, Boulanger CA, Smith GH, et al. Stem cell marker prominin-1 regulates branching morphogenesis, but not regenerative capacity, in the mammary gland. Dev Dyn. 2012; 240:674–81. [PubMed: 21337465]

Andl T, Reddy ST, Gaddapara T, Millar SE. WNT signals are required for the initiation of hair follicle development. Dev Cell. 2002; 2:643–53. [PubMed: 12015971]

Bolos V, Peinado H, Perez-Moreno MA, et al. The transcription factor Slug represses E-cadherin expression and induces epithelial to mesenchymal transitions: a comparison with Snail and E47 repressors. J Cell Sci. 2003; 116:499–511. [PubMed: 12508111]

Bull N, Johnson T, Martin K. Organotypic explant culture of adult rat retina for in vitro investigations of neurodegeneration, neuroprotection and cell transplantation. Nat Protocol Exchange. 2011 doi: 10.1038.

Byers LA, Diao L, Wang J, et al. An epithelial-mesenchymal transition gene signature predicts resistance to EGFR and PI3K inhibitors and identifies Axl as a therapeutic target for overcoming EGFR inhibitor resistance. Clin Cancer Res. 2013; 19:279–90. [PubMed: 23091115]

Chiang C, Swan RZ, Grachtchouk M, et al. Essential role for Sonic hedgehog during hair follicle morphogenesis. Dev Biol. 1999; 205:1–9. [PubMed: 9882493]

Corbeil, DenisProminin-1 (CD133): New Insights on Stem & Cancer Stem Cell Biology Series. Advs Exp Med Biol. 2013; 777:250.

Devenport D, Fuchs E. Planar polarization in embryonic epidermis orchestrates global asymmetric morphogenesis of hair follicles. Nat Cell Biol. 2008; 10:1257–68. [PubMed: 18849982]

Fargeas CA. Prominin-2 and Other Relatives of CD133. Adv Exp Med Biol. 2013; 777:25–40. [PubMed: 23161073]

Florek M, Haase M, Marzesco AM, et al. Prominin-1/CD133, a neural and hematopoietic stem cell marker, is expressed in adult human differentiated cells and certain types of kidney cancer. Cell Tissue Res. 2005; 319:15–26. [PubMed: 15558321]

Gay D, Kwon O, Zhang Z, et al. Fgf9 from dermal γδ T cells induces hair follicle neogenesis after wounding. Nat Med. 2013; 19:916–23. [PubMed: 23727932]

Groger CJ, Grubinger M, Waldhor T, et al. Meta-analysis of gene expression signatures defining the epithelial to mesenchymal transition during cancer progression. PLoS One. 2012; 7:e51136. [PubMed: 23251436]

Grosse-Gehling P, Fargeas CA, Dittfeld C, et al. CD133 as a biomarker for putative cancer stem cells in solid tumours: limitations, problems and challenges. J Pathol. 2013; 229:355–78. [PubMed: 22899341]

Heuberger J, Birchmeier W. Interplay of cadherin-mediated cell adhesion and canonical Wnt signaling. Cold Spring Harb Perspect Biol. 2010; 2:a002915. [PubMed: 20182623]

Hirata A, Utikal J, Yamashita S, et al. Dose-dependent roles for canonical Wnt signalling in de novo crypt formation and cell cycle properties of the colonic epithelium. Development. 2013; 140:66–75. [PubMed: 23222438]

Huang DW, Sherman BT, Lempicki RA. Systematic and integrative analysis of large gene lists using DAVID Bioinformatics Resources. Nature Protoc. 2009; 4:44–57. [PubMed: 19131956]

Huang DW, Sherman BT, Lempicki RA. Bioinformatics enrichment tools: paths toward the comprehensive functional analysis of large gene lists. Nucleic Acids Res. 2009; 37:1–13. [PubMed: 19033363]

Huelsken J, Vogel R, Erdmann B, et al. b-Catenin Controls Hair Follicle Morphogenesis and Stem Cell Differentiation in the Skin. Cell. 2001; 105:533–545. [PubMed: 11371349]

Humtsoe JO, Koya E, Pham E, et al. Transcriptional profiling identifies upregulated genes following induction of epithelial-mesenchymal transition in squamous carcinoma cells. Exp Cell Res. 2012; 318:379–90. [PubMed: 22154512]

Ito Y, Hamazaki TS, Ohnuma K, et al. Isolation of murine hair-inducing cells using the cell surface marker prominin-1/CD133. J Invest Dermatol. 2007; 127:1052–60. [PubMed: 17185982]

Jamora C, DasGupta R, Kocieniewski P, et al. Links between signal transduction, transcription and adhesion in epithelial bud development. Nature. 2003; 422:317–22. [PubMed: 12646922]

Jamora C, Lee P, Kocieniewski P, et al. A signaling pathway involving TGF-beta2 and snail in hair follicle morphogenesis. PLoS Biol. 2005; 3:e11. [PubMed: 15630473]

Karbanova J, Missol-Kolka E, Fonseca AV, et al. The stem cell marker CD133 (Prominin-1) is expressed in various human glandular epithelia. J Histochem Cytochem. 2008; 56:977–93. [PubMed: 18645205]

Komuve L, Hanley K, Jiang Y, et al. Induction of selected lipid metabolic enzymes and differentiation-linked structural proteins by air exposure in fetal rat skin explants. J Invest Derm. 1999; 112:303–309. [PubMed: 10084306]

Lamouille S, Xu J, Derynck R. Molecular mechanisms of epithelial-mesenchymal transition. Nat Rev Mol Cell Biol. 2014; 15:178–196. [PubMed: 24556840]

Lee J, Tumbar T. Hairy tale of signaling in hair follicle development and cycling. Sems Cell Dev Biol. 2012; 23:906–916.

Lei Z, Maeda T, Tamura A, et al. EpCAM contributes to formation of functional tight junction in the intestinal epithelium by recruiting claudin proteins. Dev Biol. 2012; 371:136–45. [PubMed: 22819673]

Litvinov SV, Velders MP, Bakker HA. Ep-CAM: a human epithelial antigen is a homophilic cell-cell adhesion molecule. J Cell Biol. 1994; 125:437–46. [PubMed: 8163559]

Litvinov SV, Balzar M, Winter MJ, et al. Epithelial cell adhesion molecule (Ep-CAM) modulates cell-cell interactions mediated by classic cadherins. J Cell Biol. 1997; 139:1337–48. [PubMed: 9382878]

Lu H, Ma J, Yang Y, Shi W, et al. EpCAM is an endoderm-specific Wnt derepressor that licenses hepatic development. Dev Cell. 2013; 24:543–53. [PubMed: 23484855]

Mak AB, Nixon AM, Kittanakom S, et al. Regulation of CD133 by HDAC6 promotes β-catenin signaling to suppress cancer cell differentiation. Cell Rep. 2012; 2:951–63. [PubMed: 23084749]

Martínez-Estrada OM, Cullerés A, Soriano FX, et al. The transcription factors Slug and Snail act as repressors of Claudin-1 expression in epithelial cells. Biochem J. 2006; 394:449–57. [PubMed: 16232121]

Mikkola ML. Genetic basis of skin appendage development. Semin Cell Dev Biol. 2007; 18:225–36. [PubMed: 17317239]

Millar SE. Molecular Mechanisms Regulating Hair Follicle Development. J Invest Dermatol. 2002; 118:216–225. [PubMed: 11841536]

Mootha VK, et al. PGC-1alpha-responsive genes involved in oxidative phosphorylation are coordinately downregulated in human diabetes. Nat Genet. 2003; 34:267–73. [PubMed: 12808457]

Müller-Röver S, Tokura Y, Welker P, et al. E- and P-cadherin expression during murine hair follicle morphogenesis and cycling. Exp Dermatol. 1999; 8:237–46. [PubMed: 10439220]

Nanba D, Hieda Y, Nakanishi Y. Remodeling of desmosomal and hemidesmosomal adhesion systems during early morphogenesis of mouse pelage hair follicles. J INVEST DERMATOL. 2000; 114:171–177. [PubMed: 10620134]

Peinado H, Olmeda D, Cano A. Snail, Zeb and bHLH factors in tumour progression: an alliance against the epithelial phenotype? Nat Rev Cancer. 2007; 7:415–28. [PubMed: 17508028]

Schneider MR, Schmidt-Ullrich R, Paus R. The Hair Follicle as a Dynamic Miniorgan. Curr Biol. 2009; 19:132–142.

Shtutman M, Levina E, Ohouo P, et al. Cell adhesion molecule L1 disrupts E-cadherin-containing adherens junctions and increases scattering and motility of MCF7 breast carcinoma cells. Cancer Res. 2006; 66:11370–80. [PubMed: 17145883]

Stepniak E, Radice GL, Vasioukhin V. Adhesive and Signaling Functions of Cadherins and Catenins in Vertebrate Development. Cold Spring Harb Perspect Biol. 2009; 1:a002949. [PubMed: 20066120]

Subramanian A, Tamayo P, Mootha VK, et al. Gene set enrichment analysis: a knowledge-based approach for interpreting genome-wide expression profiles. Proc Natl Acad Sci U S A. 2005; 102:15545–50. [PubMed: 16199517]

Surmann-Schmitt C, Widmann N, Dietz U, et al. Wif-1 is expressed at cartilage-mesenchyme interfaces and impedes Wnt3a-mediated inhibition of chondrogenesis. J Cell Sci. 2009; 122:3627–37. [PubMed: 19755491]

ten Berge D, Koole W, Fuerer C, et al. Wnt signaling mediates self-organization and axis formation in embryoid bodies. Cell Stem Cell. 2008; 3:508–18. [PubMed: 18983966]

Tinkle CL, Lechler T, Pasolli HA, et al. Conditional targeting of E-cadherin in skin: Insights into hyperproliferative and degenerative responses. Proc Nat Acad Sci. 2003; 101:552–557. [PubMed: 14704278]

Tinkle CL, Pasolli HA, Stokes N, et al. New insights into cadherin function in epidermal sheet formation and maintenance of tissue integrity. Proc Nat Acad Sci. 2008; 105:15405–15410. [PubMed: 18809908]

Trzpis M, Bremer E, McLaughlin PM, et al. EpCAM in morphogenesis. Front Biosci. 2008; 13:5050–5. [PubMed: 18508569]

Warrington SJ, Strutt H, Strutt D. The Frizzled-dependent planar polarity pathway locally promotes E-cadherin turnover via recruitment of RhoGEF2. Development. 2013; 140:1045–54. [PubMed: 23364328]

Wells KL, Mou C, Headon DJ, et al. Recombinant EDA or Sonic Hedgehog rescue the branching defect in Ectodysplasin A pathway mutant salivary glands in vitro. Dev Dyn. 2010; 239:2674–2684. [PubMed: 20803597]

Wu CJ, Mannan P, Lu M, et al. Epithelial cell adhesion molecule (EpCAM) regulates claudin dynamics and tight junctions. J Biol Chem. 2013; 288:12253–68. [PubMed: 23486470]

Zhang Y, Andl T, Yang SH, et al. Activation of beta-catenin signaling programs embryonic epidermis to hair follicle fate. Dev. 2008; 135:2161–72.

Zhu L, Gibson P, Currle DS, et al. Prominin 1 marks intestinal stem cells that are susceptible to neoplastic transformation. Nature. 2009; 457:603–7. [PubMed: 19092805]
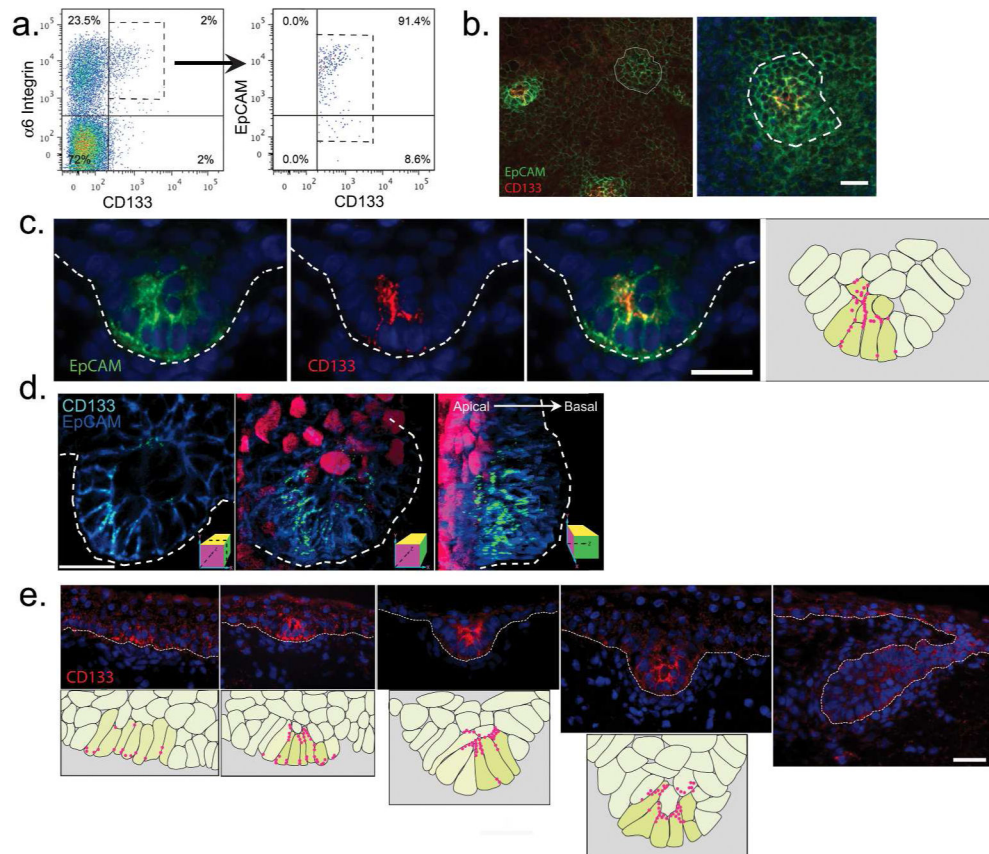
Figure 1. CD133 is an early marker of human hair follicle placodes

(a) Density dot plots of fetal scalp epidermal cells for expression of CD133 and alpha6-integrin (left) and alpha6-integrin$^+$CD133$^+$ cells for EpCAM and forward scatter (right). (b) Scalp whole mounts stained for EpCAM and CD133. Dotted line outlines CD133$^-$EpCAM$^+$ placode (left) or magnified CD133$^+$EpCAM$^+$ placode (right). (c) Frozen section of placode stained for EpCAM, CD133, overlap or schematic of CD133 localization. DAPI-stained nuclei are blue. Schematic placode cells are shaded light yellow (CD133- cells), dark yellow (CD133+ cells). The red dots represent CD133 location. (d) Single (left) and 3D stacked confocal images (middle and right) of placode stained for EpCAM and CD133. Cartoons denote orientation. Light purple nuclei in middle and right panels show DAPI-stained periderm. (e) Developing hair follicles analyzed for CD133 expression with schematic representations below. Scale bars are 25 μm. (a) – (e) N = 12 and N(t) = 6 (where N means the number of times these experiments were done and N(t) = number of individual tissue samples analyzed.
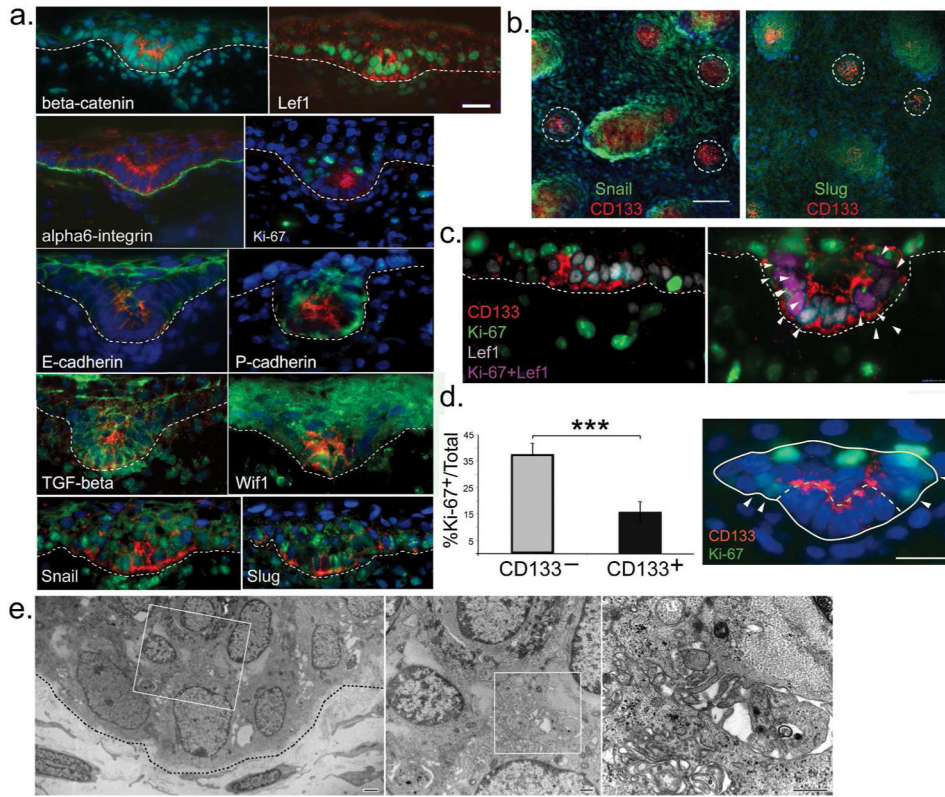
Figure 2. CD133 expression correlates with Wnt activation and early hair morphogenesis but not proliferation

(a) Frozen sections of placodes co-stained for CD133 (red) and labeled markers (see panels). DAPI-stained nuclei are blue. Scale bar 25 μm. (b) Stacked confocal images of fetal scalp epidermis whole mounts stained for Snail or Slug and CD133. White dotted lines outline placodes. Scale bar 75 μm. (c) Triple staining of frozen sections for CD133, Lef1 and Ki-67. White arrows denote locations of Lef1:Ki-67 double-positive cells (right). Scale bar 25 μm. (a) – (c) N and N(t) = 3. (d) Bar graph comparing percent Ki-67$^+$ cells within CD133$^-$ and CD133$^+$ populations. Data are means ± SEM, ***$P < 0.005$. Example of compared regions (right). Arrows indicate Ki-67$^+$ cells adjacent to CD133$^+$ cells. Scale bar 25 μm. N = 22 placodes analyzed and N(t) = 3. (e) TEM analysis of 12 week placode. Rectangles show areas of magnification left to right. Scale bars; left, 2 μm; others, 500 nm. N and N(t) = 4.
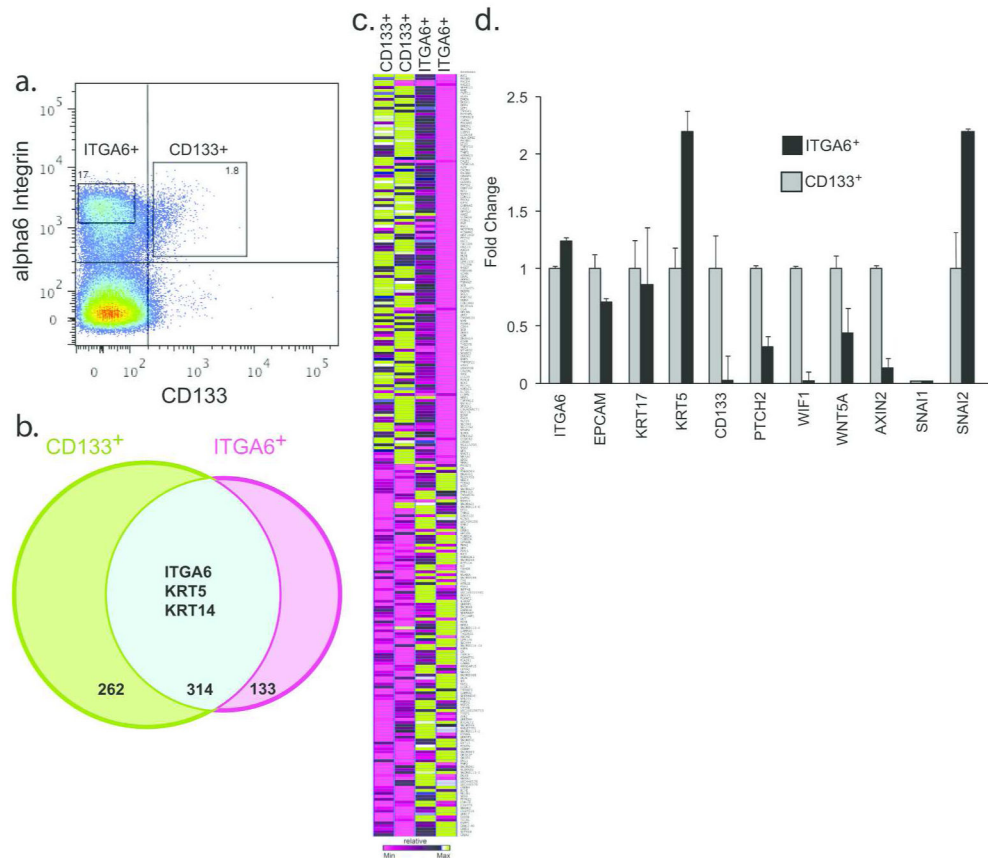
Figure 3. CD133+ cells express genes indicative of early hair follicle placode morphogenesis and EMT

(a) Representative dot plot of 13 week fetal scalp epidermal populations. Squares define regions of ITGA6+ and CD133+ sorted populations. (b) Venn diagram comparing overlap of gene expression in ITGA6+ and CD133+ populations. (c) Heatmap comparing differentially expressed genes in ITGA6+ and CD133+ populations from two independent array analyses. Green denotes upregulated and pink downregulated genes. N and N(t) = 2 arrays from 2 independent sorts. Results represent merged analyses (d) QPCR analyses comparing transcription levels of specific genes in sorted ITGA6+ (black bars) and CD133+ (gray bars) populations as described in Gay et al, 2013. N and N(t) = 3.
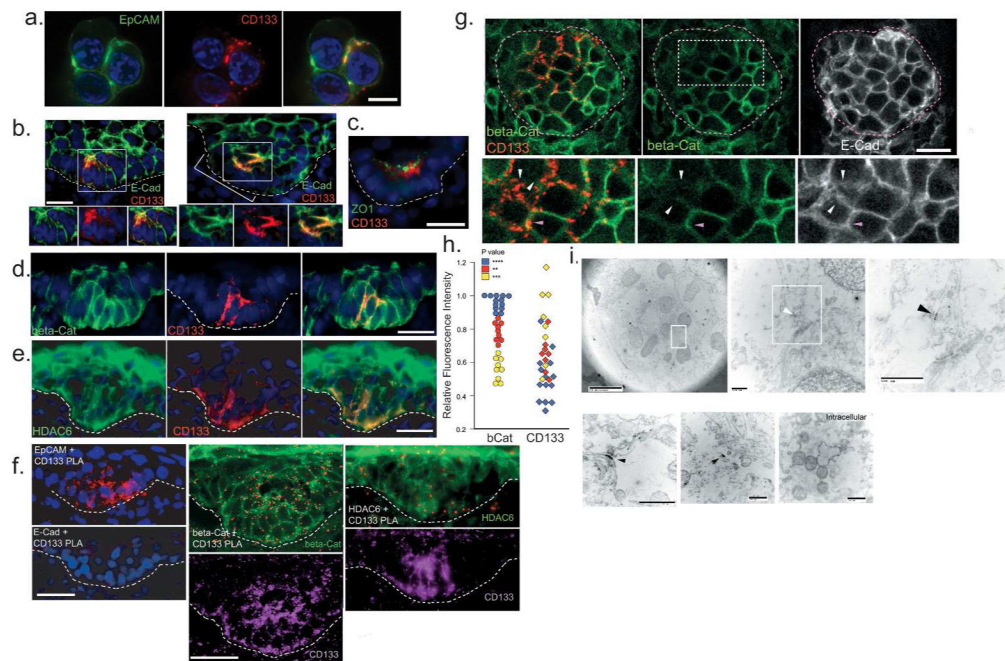
Figure 4. CD133 localizes to AJs in early placodes and to regions of beta-catenin and E-cadherin down-regulation in later placodes

(a) IF image of sub-placode cluster, dissociated from surrounding interfollicular epidermis, stained for CD133 and EpCAM. Scale bar 5 μm. (b) IF images of early (left) and later (right) placodes stained for CD133 and E-cadherin. Line (right panel) indicates E-cadherin-depleted region. Squares indicate magnified areas (lower panels). (c) – (e) IF of placode stained for CD133 and ZO1 (c), beta-catenin (d), HDAC6 (e). (f) In situ PLA of 'CD133 + EpCAM', 'CD133 + E-cadherin', 'CD133 + beta-catenin ' and 'CD133 + HDAC6' antibody combinations. Placodes in middle and right panels were counter-stained for beta-catenin or HDAC6 respectively and CD133. Scale bars 25 μm in (b) – (f). (g) Stacked confocal images of a placode co-stained for CD133, beta-catenin and E-cadherin. Rectangle defines magnified regions (lower panels). White arrowheads indicate regions of high CD133 and low beta-catenin and E-cadherin localization. Pink arrowhead indicates co-localized proteins. Scale bar 10 μm. (h) Scatter plot comparing relative fluorescence intensities of betacatenin and CD133 proteins along placode cell membranes. Left side shows relative fluorescence of membranes for beta-catenin (bCat): blue (high), red (intermediate) and yellow (low). Right side compares CD133 fluorescence within each group. See Fig S6 for details. N = 31 regions from 8 placodes. N(t) = 3. **P < 0.01, ***P < 0.005, ****P < 0.001. (i) IFTEM of CD133 localization in placodes. Boxed regions show increased magnification left to right. Bottom panels provide additional examples. Arrowheads point to regions with high immunogold content. Scale bar middle left panel 10 μm, all other panels 500 nm. (a) – (i) N and N(t)   3.
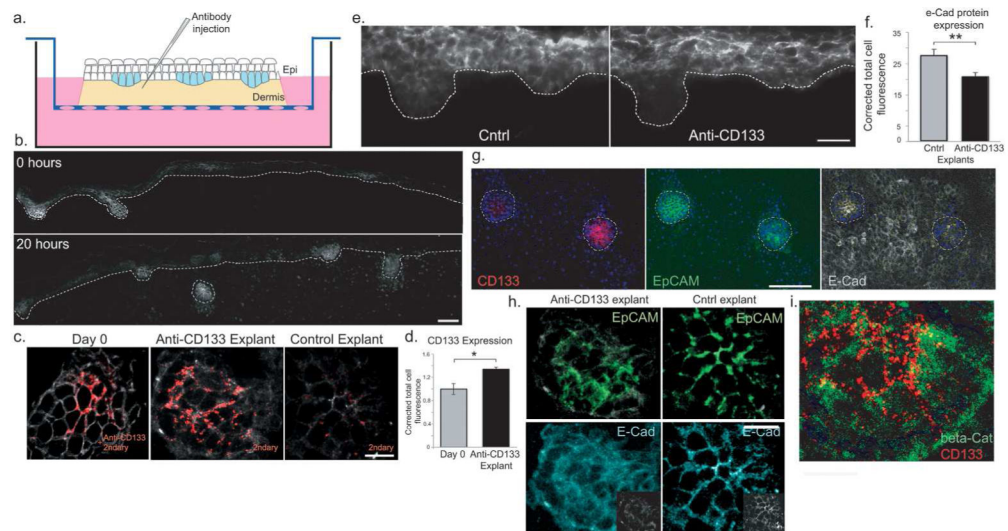
Figure 5. Perturbation of CD133 protein drives accelerated E-cadherin membrane loss in scalp explant placodes

(a) Schematic depicting scalp explant. (b) IF images of Day 0 (top) and 20 hour explant (bottom) stained for EpCAM. Scale bar 50 μm. (c) Confocal images comparing Day 0 scalp (stained with anti-CD133 and secondary antibodies, left panel) with anti-CD133 (middle) and control (right) explants stained with secondary antibodies only. (d) Bar graph showing relative CD133 protein concentration in Day 0 and anti-CD133 explant placodes and germs. N = 9 placodes for each group. (e) IF of Cntrl and anti-CD133 explants stained for E-cadherin. Scale bar 25 μm. (f) Bar graph showing quantitative comparison of E-cadherin in control and anti-CD133 explant placodes and germs. N = 18 placodes for each group. (g) Confocal image of adjacent placodes in anti-CD133 explant stained with secondary (CD133, red), EpCAM and E- cadherin antibodies. Scale bar 75 μm. (h) Confocal images of placodes from anti-CD133 and Cntrl explants stained for EpCAM (top) and E-cadherin (bottom). Insets in E-cad panels show true unenhanced intensities. (i) Confocal image from an anti-CD133 explant stained with secondary (red) and beta-catenin antibodies. Scale bars 10 μm (c, h, i). Data are means ± SEM, *$P < 0.05$, **$P < 0.01$. (a) – (i) N and N(t) 3.
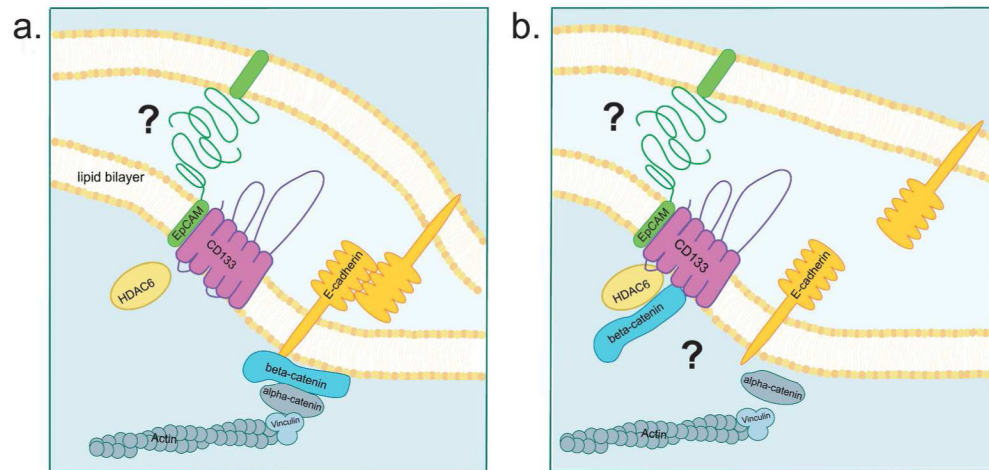
Figure 6. Hypothetical model for the role of CD133 in AJ loss during human hair follicle placode morphogenesis

(a) Schematic representation of an AJ connecting intercellular membranes. (b) Proposed model of AJ disruption following CD133 association with AJ beta-catenin protein. It should be noted that CD133 colocalization with AJ proteins prior to loss their loss in CD133-rich regions (Fig 4) indicates a time lag that may point to a more complex phenomenon than the simple model proposed here. EpCAM association with CD133 and possible transient association of HDAC6 with CD133 reflect results from PLA analyses in a. 4. Weak homophilic intercellular interaction between EpCAM proteins has been demonstrated by Litvinov et al, 1994. The question marks for EpCAM:EpCAM interaction (panel A) and CD133 sequestration of membrane beta-catenin (panel B) denote that these possibilities remain hypothetical.

Table I

Microarray results of differentially regulated and unaffected genes in CD133^{+} cells compared with ITGA6^{+} cells.

	CD133^{+} population: Up-regulated Genes
Signaling pathways: Target genes	**WNT:** WIF1, DKK4, LGR5, WNT5A **SHH:** PTCH2 **EDA:EDAR:** EDAR **TGF:** TGFB2, BMP5 **Others;** BDNF, FGF20, TNFS10
Cell Motility and Morphogenesis (DAVID[1])	CD34, VAV3, SELE, CXCR4, DCLK1, FLT1, KDR, NRP1, NRP2, TGFB2, VCAN, BDNF, KIF5C, LIFR
Downstream targets of EMT (signaling pathways, cell motility and unknownfunctions)(Groger et al, 2012[2];Humtsoe et al, 2012; Byers et al, 2013)	TGFB2, WNT5A, ETV5, VCAN, NRP2, ADAM23, CLD1, A2M, HAS2, GNG11, MSX2, SCUBE3, MYB, MCCT1, NRSA2, BDNF, NRP1, VAV3 FRZB, CDH11, PAPSS2, SLC27A2
Mammary Stem Cell Gene Set (GSEA M2573)	PRDM1, WIF1, LIFR, DUSP6, NRP1, GNGL1, MICAL2, NRP2, COL14A1, MME, ETV5, KCNMA1, HAS2, MYB, LRRN1, KDELC1
	CD133^{+} population: Unaffected Genes
EMT downmodulators of eCadherin (Lamouille et al, 2014)	SNAI1, SNAI2, ZEB1, TCF3, TCF4, KLF8, TWIST, SIX1, FOXC2, FOXF1, FOXD3, FOXQ1, FOXA1, FOXA2, GATA4, GATA6, HMGA2, ZNF703, PRX1
Down-regulated genes During EMT (Lamouille et al, 2014)	GRHL2, ELF3, ELF4
EMT targets (Lamouille et al, 2014)	CHD1, CDH2, FN1, VIM
	CD133^{+} population: Down-regulated Genes
Adhesion and Cell Junctions (DAVID)	FAT2, CDH19, LAMB4, GPNMB, LSAMP, NRXN1, POSTN, PLXNC1, DSG1, EPB4IL3, FMN1, GABRA2, GABRA4, GABRE, GRIA2, GRID2, GRIK1, LRRC7, PMP22, NLGN1
Gated Channel Activity (DAVID)	GABRA2, GABRA4, GABRE, GRIA2, GRID2, GRIK1, NMUR2, KCNJ5, RYR2, TRPC6
Pigmentation (DAVID)	DCT, EDNRB, PAX3, KIT, TYR, TYRP1
EMT downmodulators of eCadherin (Lamouille et al, 2014)	ZEB2

[1]Bioinformatics programs and references are defined in Materials and Methods.

[2]References are provided in left column in parentheses.